Acta Crystallographica Section D
Biological Crystallography
ISSN 0907-4449

Structure of the apo decarbamylated form of 2,3-diketo-5-methylthiopentyl-1-phosphate enolase from *Bacillus subtilis*

Haruka Tamura,[a] Yohtaro Saito,[b] Hiroki Ashida,[b] Yasushi Kai,[c] Tsuyoshi Inoue,[a,d] Akiho Yokota[b] and Hiroyoshi Matsumura[a,d]*

[a]Department of Applied Chemistry, Graduate School of Engineering, Osaka University, 2-1 Yamadaoka, Suita, Osaka 565-0871, Japan, [b]Department of Molecular Biology, Graduate School of Biological Science, Nara Institute of Science and Technology (NAIST), 8916-5 Takayama, Ikoma, Nara 630-0101, Japan, [c]Department of Environmental Biotechnological Future Engineering, Fukui University of Technology, 3-6-1 Gakuen, Fukui 910-8505, Japan, and [d]CREST (Sosho Project), JST, 2-1 Yamadaoka, Suita, Osaka 565-0871, Japan

Correspondence e-mail: matsumura@chem.eng.osaka-u.ac.jp

Received 27 December 2008
Accepted 12 June 2009

PDB Reference: 2,3-diketo-5-methylthiopentyl-1-phosphate enolase, 2zvi, r2zvisf.

2,3-Diketo-5-methylthiopentyl-1-phosphate enolase (DK-MTP-1P enolase), a RuBisCO-like protein (RLP), catalyzes the enolization of 2,3-diketo-5-methylthiopentyl-1-phosphate. The crystal structure of the apo decarbamylated form (E form) of *Bacillus subtilis* DK-MTP-1P enolase (Bs-DK-MTP-1P enolase) has been determined at 2.3 Å resolution. The overall structure of the E form of Bs-DK-MTP-1P enolase highly resembles that of *Geobacillus kaustophilus* DK-MTP-1P enolase (Gk-DK-MTP-1P enolase), with the exception of a few insertions or deletions and of a few residues at the active site. In the E form of Bs-DK-MTP-1P enolase, Lys150 (equivalent to Lys175 in RuBisCO) at the active site adopts a conformation that is distinct from those observed in the other forms of Gk-DK-MTP-1P enolase. This unusual conformational change appears to be induced by changes in the φ and ψ angles of Gly151, which is conserved in the sequences of the Bs-DK-MTP-1P and Gk-DK-MTP-1P enolases but not in those of RuBisCOs. The loop at 303–312, equivalent to the catalytic loop termed 'loop-6' in RuBisCO, is in a closed conformation in the E form of Bs-DK-MTP-1P enolase. The closed conformation appears to be stabilized by Pro312, which is conserved in the sequences of several RLPs (equivalent to Glu338 in RuBisCO). Based on these results, the characteristic structural features of DK-MTP-1P enolase are discussed.

1. Introduction

D-Ribulose-1,5-bisphosphate carboxylase/oxygenase (RuBisCO; EC 4.1.1.39) catalyzes the initial steps of photosynthetic CO_2 assimilation and photorespiratory carbon oxidation (Lorimer, 1981*a*). In the carboxylation reaction, one molecule each of CO_2 and H_2O are added to a five-carbon sugar phosphate, D-ribulose-1,5-bisphosphate (RuBP), to produce two molecules of 3-phosphoglycerate (3PGA; Fig. 1*a*; Andrews & Lorimer, 1987; Hartman & Harpel, 1994). In the oxygenation reaction, the enzyme utilizes O_2 instead of CO_2 to yield one molecule each of 3PGA and 2-phosphoglycolate. However, the enzyme has an extremely slow rate of catalysis, with a very low turnover rate (1–11 per second per active site; Cleland *et al.*, 1998; Badger & Bek, 2008). To exhibit carboxylation and oxygenation, the active site of RuBisCO must be activated *via* covalent carbamylation of Lys201 at the active site and subsequent coordination with Mg^{2+}. The carboxylation mechanism of RuBisCO can be divided into three partial reactions: (i) base-catalyzed enolization by abstraction of a proton from C3 of RuBP to form a 2,3-enediol intermediate, (ii) addition of CO_2 to the 2,3-enediolate intermediate to yield 2′-carboxy-3-keto-D-arabinitol-1,5-bisphosphate (2C3KABP)

and (iii) hydrolysis of 2C3KABP to form two molecules of 3PGA (Cleland *et al.*, 1998). In the enolization of RuBP by RuBisCO, the carbamate group of the carboxylated Lys201 is the base that abstracts a proton from C3 of RuBP (Cleland *et al.*, 1998).

Based on amino-acid sequences and structures, RuBisCOs can be classified into three forms, referred to as forms I, II and III. Structures of form I RuBisCOs have been extensively studied in various forms: an apo decarbamylated form (E form; Curmi *et al.*, 1992; Schneider *et al.*, 1990), a carbamylated form complexed with Mg^{2+} (ECM form; Lundqvist & Schneider, 1991*b*; Taylor & Andersson, 1997*b*), a decarbamylated form complexed with PO_4^{3-}/SO_4^{2-} (E-PO_4^{3-}/SO_4^{2-} form; Duff *et al.*, 2000; Hansen *et al.*, 1999; Okano *et al.*, 2002; Suh *et al.*, 1987), a decarbamylated form complexed with RuBP/4CABP/XuBP (E-RuBP/4CABP/XuBP form; Newman & Gutteridge, 1993; Taylor & Andersson, 1997*a*; Taylor *et al.*, 1996; Zhang *et al.*, 1994) and a carbamylated form complexed with Mg^{2+} and RuBP/2CABP (ECM-RuBP/2CABP form; Andersson, 1996; Lundqvist & Schneider, 1991*a*; Mizohata *et al.*, 2002; Newman & Gutteridge, 1994; Shibata *et al.*, 1996; Sugawara *et al.*, 1999; Taylor *et al.*, 2001). Two flexible loops, called loop-6 and the 60s loop, have been observed to partition between 'open' and 'closed' conformations (Duff *et al.*, 2000; Saunders *et al.*, 2003; Schneider *et al.*, 1992) that determine the solvent accessibility of the active site (Schreuder *et al.*, 1993). The various RuBisCO structures have shown at least three structural combinations of the two loops: both loop-6 and the 60s loop in open conformations are observed in the E and E-PO_4^{3-}/SO_4^{2-} forms, both in closed conformations are observed in the E-RuBP/4CABP/XuBP and ECM-RuBP/2CABP forms and loop-6 in an open conformation and the 60s loop in a closed conformation are observed in the ECM form. An exception has been found for the E-SO_4^{2-} form of a form I RuBisCO from a red algae, *Galdieria partita*, which exhibits a high specificity for CO_2 fixation and adopts loop-6 in a closed conformation and the 60s loop in an open conformation (Okano *et al.*, 2002).

Many genome projects have revealed that proteins with homology to large subunits of RuBisCO may be present in bacteria, including *Bacillus subtilis* (Kunst *et al.*, 1997). These RuBisCO homologues are called RuBisCO-like proteins (RLPs) because they do not catalyze either carboxylation or oxygenation (Ashida *et al.*, 2003, 2005; Hanson & Tabita, 2001). Phylogenetic analysis indicates that RLPs may be further classified into at least three groups (RLP-α, RLP-β and RLP-γ; Ashida *et al.*, 2008; Tabita *et al.*, 2008). More recently, the biological functions and structures of RLPs have become available. RLPs from *B. subtilis* (Bs), *Geobacillus kaustophilus* (Gk) and *Microcystis aeruginosa* (Ma), all of which belong to RLP-α, have been characterized as 2,3-diketo-5-methylthiopentyl-1-phosphate enolases (DK-MTP-1P enolases; Ashida *et al.*, 2003; Carre-Mlouka *et al.*, 2006; Imker *et al.*, 2007). DK-MTP-1P enolase catalyzes the enolization of 2,3-diketo-5-methylthiopentyl-1-phosphate (DK-MTP-1P; Fig. 1*b*) and functions in the methionine-salvage pathway, which salvages methionine from methylthioadenosine (Winans & Bassler, 2002). Another RLP from *Rhodospirillum rubrum*, which also belongs to RLP-α, has been identified as a 5-methylthio-D-ribulose-1-phosphate isomerase in a new, as yet uncharacterized, pathway for sulfur salvage (Imker *et al.*, 2008). The molecular functions of the other RLPs remain unknown, although crystal structures have been solved for RLPs from *Chlorobium tepidum* and *Rhodopseudomonas palustris*, both of which belong to RLP-γ (Li *et al.*, 2005; Tabita *et al.*, 2007).

Imker and coworkers have reported the crystal structures of four different forms of Gk-DK-MTP-1P enolase (60% sequence identity with Bs-DK-MTP-1P enolase; Imker *et al.*, 2007): a PO_4^{3-}-bound decarbamylated form (E-PO_4^{3-}; PDB code 2oej), a carbamylated (activated) form complexed with Mg^{2+} (ECM; PDB code 2oek), a carbamylated form com-

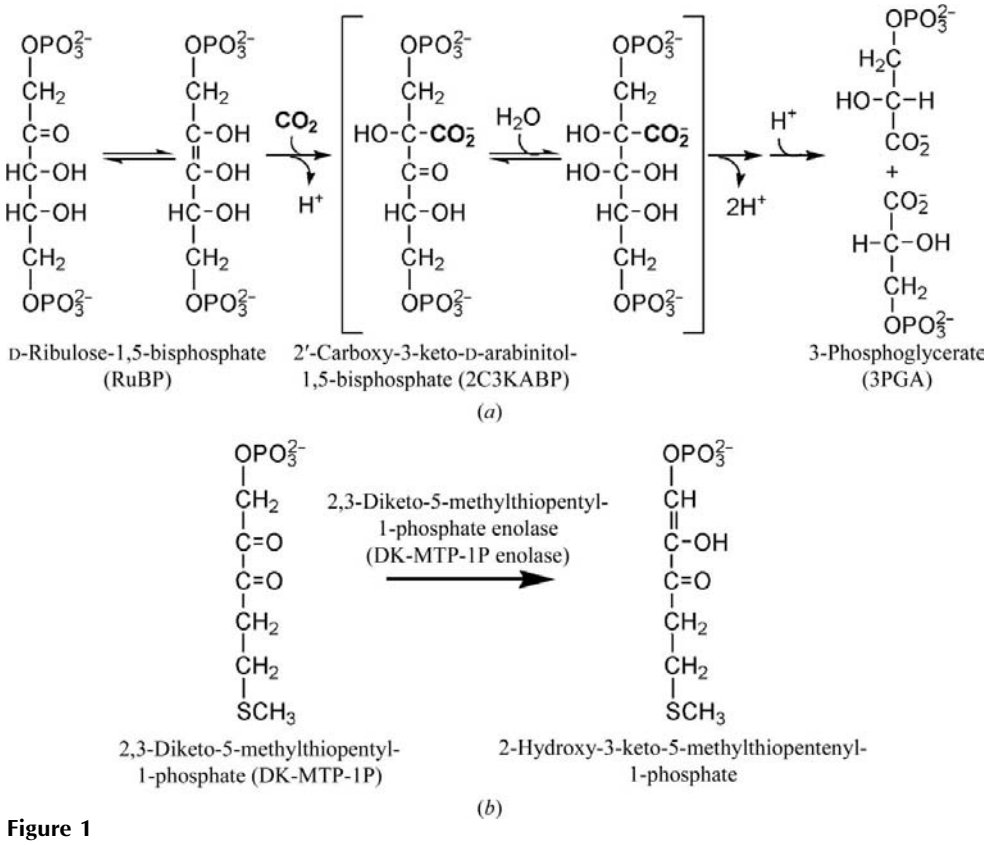

Figure 1
(*a*) The carboxylation reaction catalyzed by RuBisCO. (*b*) The enolization reaction catalyzed by 2,3-diketo-5-methylthiopentyl-1-phosphate enolase.

Table 1
Data-collection and refinement statistics.

Values in parentheses are for the highest resolution shell (2.42–2.30 Å).

Beamline	SPring-8 BL44XU
Space group	$P2_1$
Unit-cell parameters (Å, °)	a = 79.3, b = 91.5, c = 107.0, β = 90.8
Resolution range (Å)	30.5–2.30
No. of molecules per ASU	4
V_M (Å^3 Da^{-1})	2.2
V_{solv} (%)	43
No. of measured reflections	259484
No. of unique reflections	64719
$I/\sigma(I)$	7.2 (2.4)
R_{merge}† (%)	8.4 (27.3)
Completeness (%)	95.0 (95.3)
R_{work} (%)	20.1
R_{free} (%)	24.2
R.m.s. deviations	
Bonds (Å)	0.006
Angles (°)	1.4
Ramachandran statistics, residues in	
Most favoured region (%)	88.1
Additionally allowed region (%)	11.3
Generally allowed region (%)	0.6
Disallowed region (%)	0.0

† $R_{merge} = \sum_{hkl}\sum_i |I_i(hkl) - \langle I(hkl)\rangle| / \sum_{hkl}\sum_i I_i(hkl)$, where $I_i(hkl)$ is the value of the ith measurement of the intensity of a reflection, $\langle I(hkl)\rangle$ is the mean value of the intensity of that reflection and the summation is over all measurements.

plexed with Mg^{2+} and bicarbonate (ECM-HCO_3^-; PDB code 2oel) and a carbamylated form complexed with Mg^{2+} and the alternate substrate 2,3-diketohexane-1-phosphate (DK-H-1P; ECM-substrate; PDB code 2oem). Based on these structural and biochemical studies (Imker *et al.*, 2007), the enzyme is activated *via* carbamylation of Lys173 (equivalent to Lys201 in RuBisCO) at the active site and coordination with Mg^{2+}. DK-MTP-1P enolase is therefore considered to share the same activation mechanism as RuBisCO (Lorimer, 1981*b*; Lorimer *et al.*, 1993; Lorimer & Miziorko, 1980; Miziorko & Sealy, 1980; Pierce & Reddy, 1986). As for the open–closed transition of loop-6 and the 60s loop, the E-PO_4^{3-}-form of Gk-DK-MTP-1P enolase has both loop-6 and the 60s loop in open conformations, while the other three forms (ECM, ECM-HCO_3^- and ECM-substrate) have loop-6 in a closed conformation and the 60s loop in an open conformation. Whereas structures of each form (E, ECM and ECM-ligand) of RuBisCOs are presently available, the crystal structure of the apo decarbamylated form (E) of DK-MTP-1P enolase remains unknown. If structural information for the E form of DK-MTP-1P enolase is available, dynamic events that occur in the discrete catalytic steps may be elucidated. In addition, structure comparison with RuBisCO in the same enzymatic state will allow structural clarification of the consistency between DK-MTP-1P enolase and RuBisCO, which may provide clues to the functional and evolutionary relationships between RLPs and RuBisCO.

Here, we present the crystal structure of the E form of Bs-DK-MTP-1P enolase. In the structure, the conformation of Lys150 (equivalent to Lys175 in RuBisCO) differs from those of the other forms of Gk-DK-MTP-1P enolase. This unique conformational change is accompanied by changes in the φ and ψ angles of Gly151, which is conserved in the sequences of Bs-DK-MTP-1P and Gk-DK-MTP-1P enolases. Unlike the E form of RuBisCO, in the E form of DK-MTP-1P enolase the loop at 299–311 (equivalent to loop-6 in RuBisCO) is in a closed conformation and the loop at 37–46 (equivalent to the 60s loop) is positioned about 15 Å away from the active site. These structural features provide insights into potential functional differences between RLPs and RuBisCO.

2. Experimental procedures

2.1. Crystallization and data collection

DK-MTP-1P enolase from *B. subtilis* (Bs-DK-MTP-1P enolase) was overexpressed in *Escherichia coli* and purified according to a previously reported method (Ashida *et al.*, 2003). In this study, we aimed to solve the crystal structure in the apo decarbamylated form (E form) by preparing the buffer solution containing 1 m*M* EDTA. Bs-DK-MTP-1P enolase was crystallized using the hanging-drop vapour-diffusion method at 293 K (Tamura *et al.*, 2009). The crystallographic and X-ray data statistics are summarized in Table 1.

The crystals were flash-cooled in cryoprotectant [20%(*v*/*v*) glycerol]. Diffraction data were collected on beamline BL44XU at SPring-8. The crystals belonged to space group $P2_1$, with unit-cell parameters a = 79.3, b = 91.5, c = 107.0 Å, β = 90.8°. Diffraction data were processed with the *MOSFLM* program (Leslie, 2006) and the *CCP*4 program suite (Collaborative Computational Project, Number 4, 1994).

2.2. Structural determination and refinement

The structure of Bs-DK-MTP-1P enolase was determined by the molecular-replacement method using the program *MOLREP* (Vagin & Teplyakov, 1997), with the structure of the carbamylated form of the DK-MTP-1P enolase from *G. kaustophilus* (PDB code 2oek) as a search model. Refinement procedures for Bs-DK-MTP-1P enolase were carried out using the program *CNS* (Brünger *et al.*, 1998) without non-crystallographic symmetry (NCS) restraints/constraints. The structures were visualized and modified using the programs *O* (Jones *et al.*, 1991) and *Coot* (Emsley & Cowtan, 2004). The final R_{work} and R_{free} were 20.1% and 24.2% for the E form of Bs-DK-MTP-1P enolase at 2.3 Å resolution. The electron-density map was clear for almost the entire polypeptide of Bs-DK-MTP-1P enolase. The stereochemical qualities of the final structures were assessed using the program *PROCHECK* (Laskowski *et al.*, 1993). The figures were generated using *MOLSCRIPT* (Kraulis, 1991) and *RASTER3D* (Merritt & Murphy, 1994) and all structural comparisons were carried out using the program *LSQKAB* (Collaborative Computational Project, Number 4, 1994).

3. Results and discussion

3.1. Overall structure

The final model of the apo decarbamylated form (E form) of Bs-DK-MTP-1P enolase contained two dimers in the asymmetric unit of the crystal (residues 11–22, 25–66 and 70–

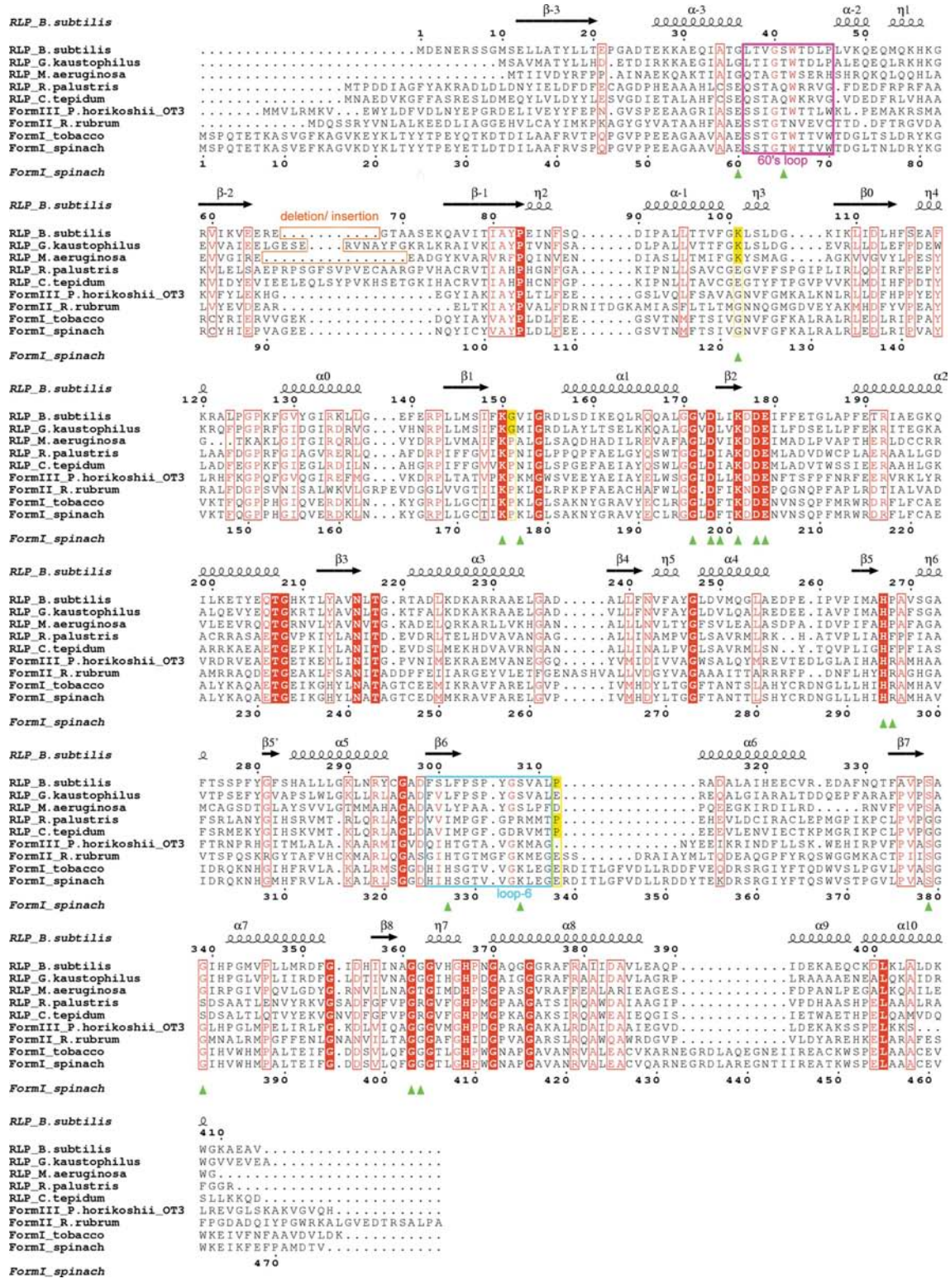

Figure 2
Sequence alignment of *Bacillus subtilis* DK-MTP-1P enolase and homologous proteins. The sequences are five RLPs from *B. subtilis* (NP_389242), *Geobacillus kaustophilus* (YP_146806), *Microcystis aeruginosa* PCC 7806 (CAJ43366), *Rhodopseudomonas palustris* (NP_947514) and *Chlorobium tepidum* (NP_662651) and four RuBisCOs from *Pyrococcus horikoshii* OT3 (form III; NP_142861.1), *Rhodospirillum rubrum* (form II; YP_427487), tobacco (form I; NP_054507) and spinach (form I; NP_054944). The numbers above the sequences as well as the secondary-structure assignments refer to Bs-DK-MTP-1P enolase. α-Helices, β-strands and 3_{10}-helices are denoted by the Greek characters α, β and η, respectively. The fully conserved residues are highlighted in red boxes and the red amino-acid residues are moderately conserved. The deletion region between β-2 and β-1 is highlighted with an orange box. The 60s loop and loop-6 are highlighted in magenta and cyan boxes, respectively. The numbers below the sequences refer to those of spinach RuBisCO and are used as a general position. The residues involved in the substrate binding and catalytic activity of RuBisCO are marked by green triangles. For Bs-DK-MTP-1P enolase, some key residues described in the text are highlighted in yellow.

410 of chain *A*, residues 11–66 and 72–411 of chain *B*, residues 11–39, 48–66 and 73–409 of chain *C* and residues 11–36, 46–67 and 73–413 of chain *D*; Fig. 3*a*). The polypeptides can be superimposed with an r.m.s. deviation of 0.48–0.97 Å for their C^{α} atoms. The alternative structures of individual polypeptides arise from differences in the crystal-packing environment. The structure of Bs-DK-MTP-1P enolase resembles those of four forms of Gk-DK-MTP-1P enolase (r.m.s. deviation of 0.59–0.87 Å), except for the insertion of nine residues (residues 1–9) at the N-terminus, a deletion between residues 65 and 72 (Figs. 2, 3*b* and 3*c*) and a few residues at the active site, as discussed below. These insertions and deletions are between secondary-structure elements and are presumably not implicated in catalysis. In analogy with Gk-DK-MTP-

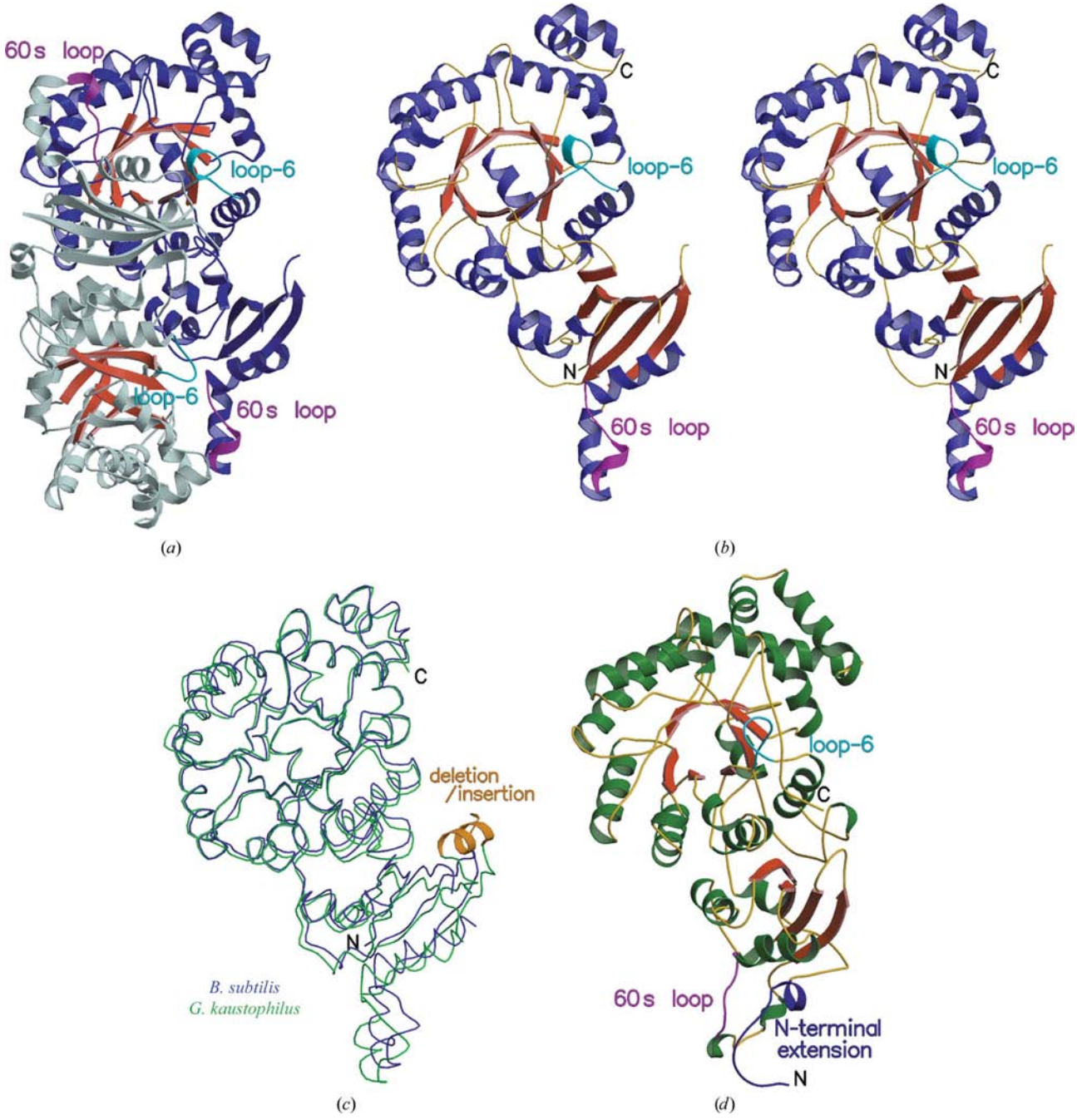

Figure 3
Structural comparisons of DK-MTP-1P enolase and RuBisCO. (*a*) Dimer structure of Bs-DK-MTP-1P enolase. The active site is located at the open end of a C-terminal $(\beta/\alpha)_8$-barrel. The barrel domain is shown in red. Loop-6 and the 60s loop are coloured cyan and magenta, respectively. (*b*) Monomer structure of Bs-DK-MTP-1P enolase in stereo. The monomer can be divided into two domains: the N-terminal domain (residues 1–143) and the C-terminal $(\beta/\alpha)_8$-barrel domain (residues 144–414). Loop-6 and the 60s loop are shown in the same colours as in (*a*). (*c*) Superposition of the C^{α} backbones of Bs-DK-MTP-1P enolase (blue) and Gk-DK-MTP-1P enolase (green; PDB code 2oem). The deletion or insertion region is shown as an orange-coloured cartoon diagram. (*d*) Monomer structure of RuBisCO from spinach (PDB code 8ruc). An N-terminal extension, which is lacking in DK-MTP-1P enolase, is coloured blue. Loop-6 and the 60s loop are shown in the same colours as in (*a*).

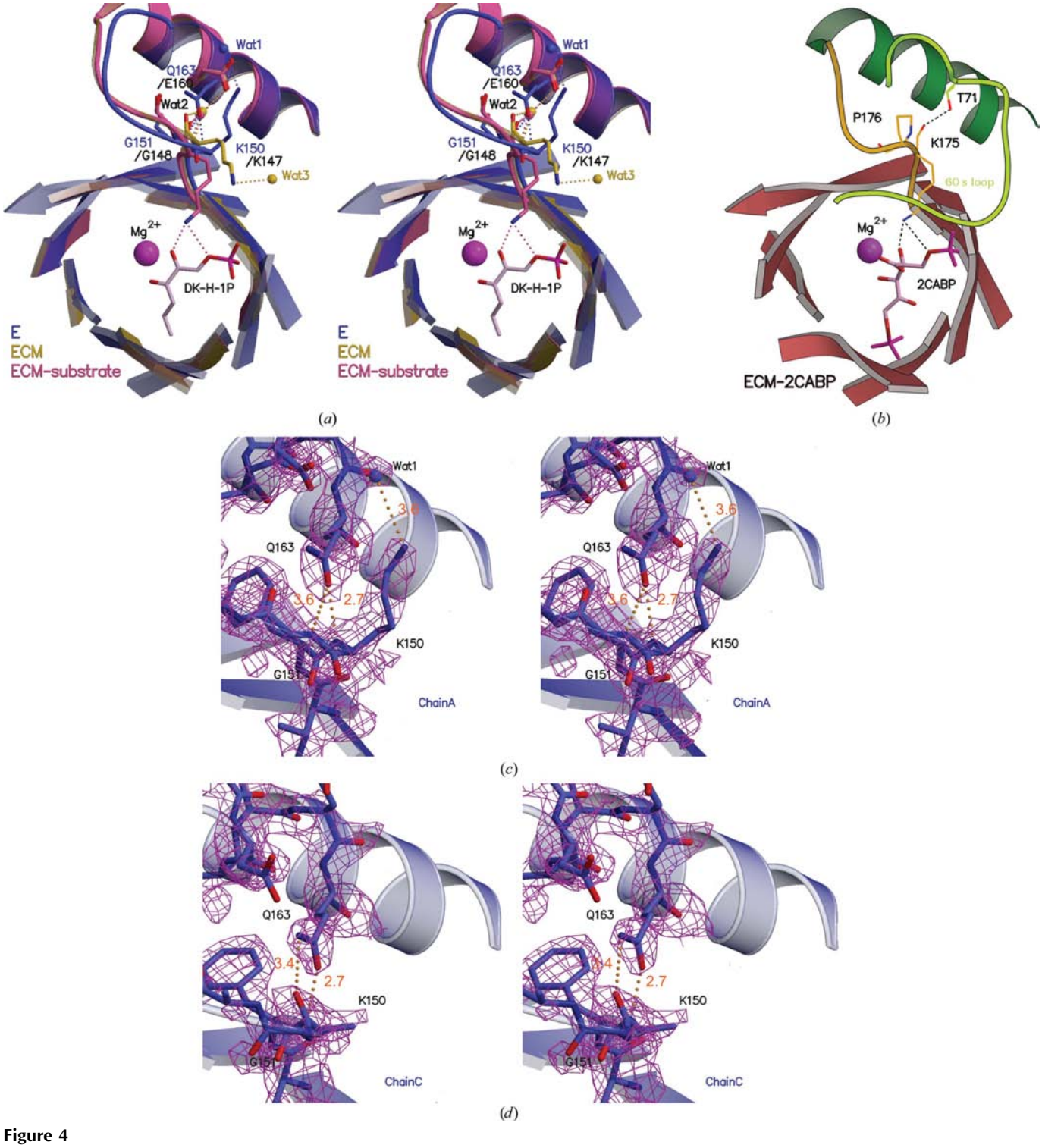

Figure 4
Active-site structures of DK-MTP-1P enolase and RuBisCO. (*a*) The inactivated form (E) of Bs-DK-MTP-1P enolase is coloured blue. The activated unliganded form (ECM) of Gk-DK-MTP-1P enolase (PDB code 2oek) is shown in yellow and the ligand-bound form with the alternate substrate 2,3-diketohexane-1-phosphate (DK-H-1P; ECM-substrate; PDB code 2oem) is shown in magenta. Neither Lys147 of E-PO_4^{3-} nor ECM-ligand are shown here, since the Lys of E-PO_4^{3-} (PDB code 2oej) adopts a similar conformation to that of ECM-ligand and the Lys of ECM-HCO_3^- (PDB code 2oel) shows a similar orientation to that of the ECM form. The structures are superimposed *via* their $(\beta/\alpha)_8$-barrel domains. The side chains of residues involved in conformational change are shown as sticks, with O atoms in red and N atoms in dark blue. The water molecules which are involved in the conformational change of Lys150 (Lys147 in *G. kaustophilus*) are shown as CPK in the same colour as each form. Hydrogen bonds are shown as dashed lines and coloured the same as each form. (*b*) The structure of spinach RuBisCO in complex with the transition-state analogue 2-carboxy-D-arabinitol-1,5-bisphosphate (2CABP; ECM-2CABP; PDB code 8ruc) is coloured as in Fig. 3(*d*). The 60s loops from the opposite monomers are shown as green line representations. The ligand is coloured as in (*a*). (*c*), (*d*) Enlarged view and the electron density around Lys150 in stereo for chain *A* (*c*) and chain *C* (*d*). The $F_o - F_c$ OMIT maps of Lys150 were calculated at the 2.5σ level (coloured in magenta). The hydrogen bonds are shown as orange dashed lines with lengths indicated in Å.

Table 2
Hydrogen bonds to Lys147/150 in DK-MTP-1P enolase (corresponding to Lys175 in RuBisCO).

	DK-MTP-1P enolase			RuBisCO		
Active state	Interacting atoms		Distance (Å)	Interacting atoms		Distance (Å)
E	Lys150 N	Gln163 $O^{\varepsilon1}$	2.7	Lys175 O	Thr71 $O^{\gamma1}$	2.6
	Lys175 N^{ζ}	Water1	3.6			
ECM	Lys147 (150) N	Water2	2.7	Lys175 O	Thr71 $O^{\gamma1}$	2.4
	Lys147 (150) O	Water2	3.1			
	Lys147 (150) N^{ζ}	Water3	3.5			
ECM	Lys147 (150) N	Water2	3.1	Lys175 O	Thr71 $O^{\gamma1}$	2.6
Ligand	Lys147 (150) O	Water2	2.9	Lys175 N^{ζ}	CABP O1	3.4
	Lys147 (150) N^{ζ}	Substrate O1	3.3		CABP O2	3.2
		Substrate O2	2.9			

1P enolase, the active sites are located at the interface between the open end of the C-terminal $(\beta/\alpha)_8$-barrel and the N-terminal domain of the neighbouring subunit within the dimer (Fig. 3*a*). The active site is composed of a glycine-rich region for phosphate binding (Gly339, Gly362 and Gly363), a positively charged residue (His267) and hydrophobic residues (Pro268 and Leu301), which are also structurally conserved in Gk-DK-MTP-1P enolase (Imker *et al.*, 2007).

3.2. Structural comparison with homologous proteins

The structure of Bs-DK-MTP-1P enolase most closely resembles those of RLPs from other groups (25–60% sequence identity) and of form III RuBisCOs (~30% sequence identity) and also resembles those of form I (~23% sequence identity) and form II (~23% sequence identity) RuBisCOs to some degree. E-form RLPs from *C. tepidum* (PDB code 1ykw) and *R. palustris* (PDB code 2qyg), both of which belong to RLP-γ, can be superimposed on Bs-DK-MTP-1P enolase with r.m.s.d.s of 2.2 and 2.3 Å for their 367 and 378 C^{α} atoms, respectively, excluding the insertions at the N-terminus and the loop between β-2 and β-1 (Fig. 2). The r.m.s.d. between Bs-DK-MTP-1P enolase and two forms (E, PDB code 2cwx, and E-SO_4^{2-}, PDB code 2d69) of form III RuBisCO from *Pyrococcus horikoshii* OT3 are both 2.3 Å for 380 C^{α} atoms. The r.m.s.d.s between Bs-DK-MTP-1P enolase and three forms (E, PDB code 1rld, ECM, PDB code 1aus, and ECM-2CABP, PDB code 8ruc) of form I RuBisCO from tobacco or spinach are 2.7–3.0 Å for their 377 C^{α} atoms (Fig. 3*d*); the r.m.s.d.s between Bs-DK-MTP-1P enolase and three forms (E, PDB code 5rub, ECM, PDB code 2rus, and ECM-RuBP, PDB code 9rub) of form II RuBisCO from *R. rubrum* are 3.3–3.5 Å for their 352 C^{α} atoms.

3.3. Induced fit of Lys150 to the active site upon substrate binding

In DK-MTP-1P enolase, substrate binding appears to trigger an induced-fit movement of Lys150 at the active site. Lys150 (at position 175 in Fig. 2) is completely conserved among forms I–III of RuBisCOs and RLPs and is a key residue participating in binding to the 1-phosphate group of the substrate during catalysis (Figs. 4*a* and 4*b*). The side chains of Lys150 exhibit a disordered conformation in chains *B* and *C* (Fig. 4*d*) but are ordered in chains *A* and *D*, pointing towards a water molecule in the solvent region (Fig. 4*c*). In the latter case, both the main-chain N atom of Lys150 and the main-chain O atom of Gly151 form hydrogen bonds to the side chain of Gln163 (Table 2). This induces a flip of the main-chain carbonyl group of Lys150 and a different orientation of the Lys150 side chain, pointing away from the active site, thus rendering the ligand-free active site accessible to solvent (Figs. 3*c* and 4*a*).

In contrast, in the ECM, ECM-HCO_3^- and ECM-substrate forms of Gk-DK-MTP-1P enolase both the main-chain N and C atoms of Lys147 (Lys150 in *B. subtilis*) form water-mediated hydrogen bonds to the side chain of Glu160 (Gln163 in *B. subtilis*), resulting in the side chain of Lys147 lying inside the active site (Fig. 4*a* and Table 2). The water-mediated hydrogen bonds to the main-chain atoms of Lys147 are not observed in the E-PO_4^{3-} form of Gk-DK-MTP-1P enolase; however, the side-chain conformation of Lys147 seems to be stabilized by interaction with the phosphate ion at the active site. The conformational change of Lys150 in DK-MTP-1P enolase depending on the enzymatic state is induced by changes in the φ (−153° to +58°) and ψ (+67° to +38°) angles of Gly151 (at position 176 in Fig. 2). Because this Gly is conserved in Bs-DK-MTP-1P and Gk-DK-MTP-1P enolases (but not in Ma-DK-MTP-1P enolase), the conformational change might be an event that is common to the Bs-DK-MTP-1P and Gk-DK-MTP-1P enolases.

Such a dynamic conformational change of Lys150 has never been observed for the equivalent residue (Lys175) in the structures of RuBisCO (Fig. 4*b*). One reason for this different behaviour of RuBisCO may arise from *cis*-Pro176, which is conserved in RuBisCOs (at the same position as Gly151 in *B. subtilis*). The φ and ψ angles of *cis*-proline seem to be rigidly constrained; indeed, the two angles of *cis*-Pro176 are virtually invariant (φ, −74° to −64°; ψ, +151° to +158°) in the distinct states of RuBisCO. Another reason could be the highly conserved Thr71 (or Ser71) at the carboxyl end of the 60s loop in RuBisCO. In RuBisCOs from spinach and tobacco the side chain of Thr71 interacts with carbonyl group of Lys175 and stabilizes the conformation of Lys175 (Fig. 4*b* and Table 2). Such an interaction is not observed in DK-MTP-1P enolase because DK-MTP-1P enolase lacks the Thr (or Ser) at position 71 and the 37–46 loop (equivalent to the 60s loop in RuBisCO) is located 15 Å away from the active site. Exceptions are found in some form III RuBisCOs, which do not conserve the Thr or Ser at position 71 (*e.g. P. horikoshii* RuBisCO). However, in this case Lys175 is sandwiched between Pro174 and Pro176, both of which are conserved in the sequences (*e.g. P. horikoshii*; see positions 174 and 176 in Fig. 2). The two Pro residues perhaps contribute to the conformational rigidity of Lys175. Thus, the difference in the primary and tertiary structures between RLP and RuBisCO is

likely to affect the structural properties of Lys175, which may reflect the functional differences between RLPs and RuBisCO.

3.4. Two loops equivalent to the 60s loop and loop-6 of RuBisCO

As described above, RuBisCO adopts an open or a closed conformation accompanied by large structural changes in the 60s loop and loop-6. Although DK-MTP-1P enolases have an equivalent two loops, strong correlations between the conformations of the two loops and the activation or binding states are not seen. In the E-PO_4^{3-} form of Gk-DK-MTP-1P enolase, the 60s loop is open and loop-6 is disordered, while the E form of Bs-DK-MTP-1P enolase and the other three forms (ECM, ECM-HCO_3^- and ECM-substrate) of Gk-DK-MTP-1P enolase adopt the 60s loop in an open conformation and loop-6 in a closed conformation (Fig. 5*a*). However, if we focus on available crystal structures of other RLPs, a rule for loop-6 conformation can be found in the primary and tertiary structures. The RLP structures of *B. subtilis*, *C. tepidum* and *R. palustris*, all of which have been solved as E forms, show loop-6 in a closed conformation. All three proteins also conserve Pro at position 338 in Fig. 2, which is located at the carboxyl end of loop-6 (Fig. 5*b*).

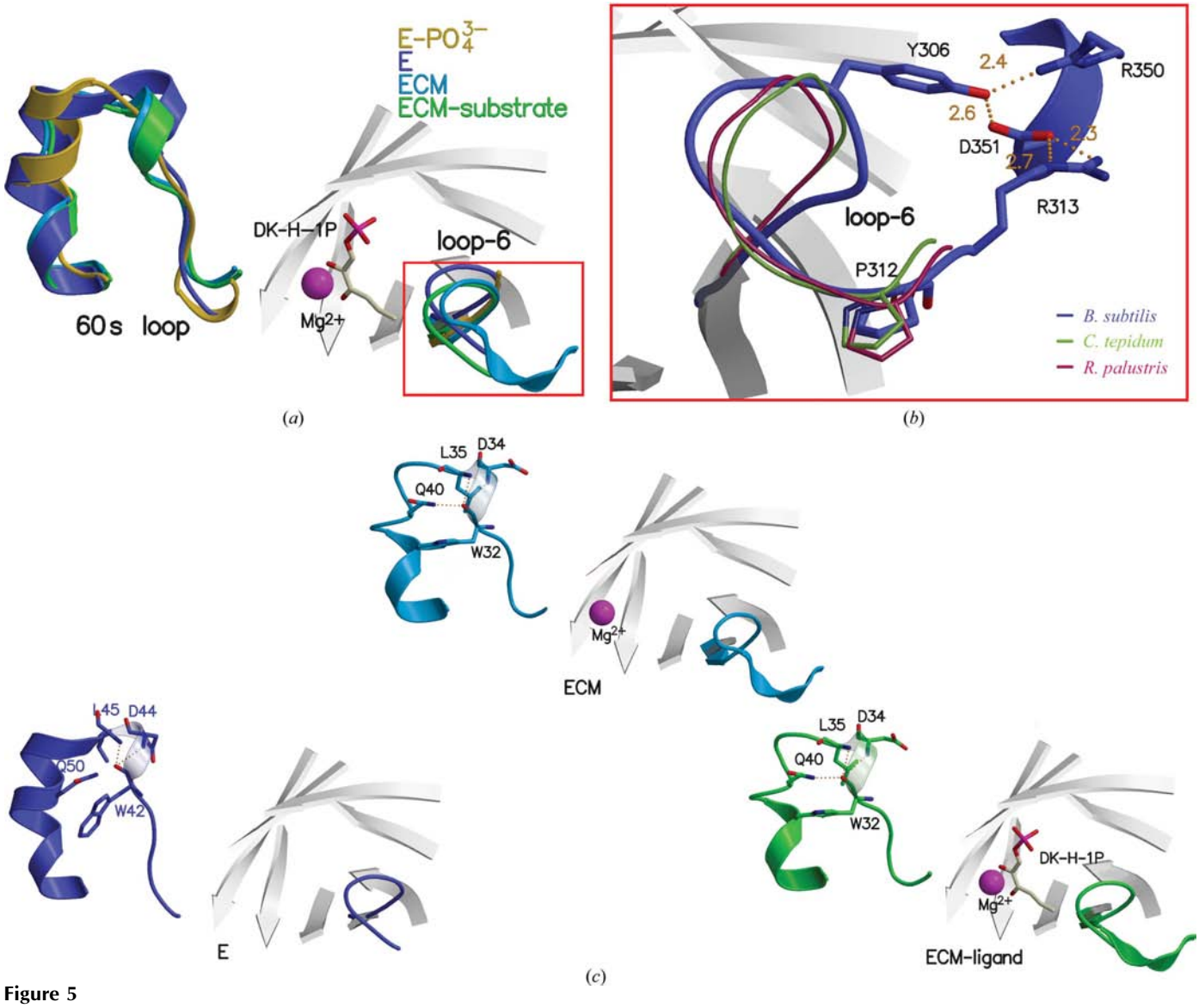

Figure 5
Structural comparison of the two loops equivalent to loop-6 and the 60s loop in DK-MTP-1P enolases. (*a*) The E form of Bs-DK-MTP-1P enolase is coloured blue and the E-PO_4^{3-} form of Gk-DK-MTP-1P enolase (PDB code 2oej) is shown in yellow. The ECM form of Gk-DK-MTP-1P enolase (PDB code 2oek) is coloured sky blue and the ligand-bound form with 2,3-diketohexane-1-phosphate (DK-H-1P; ECM-substrate; PDB code 2oem) is shown in green–yellow. (*b*) Enlarged view of loop-6 in Bs-DK-MTP-1P enolase and superpositions of loop-6 with those of the *C. tepidum* and *R. palustris* enzymes. The side chains of the residues involved in hydrogen bonds or structural stabilization are shown as sticks with O atoms in red and N atoms in dark blue. Hydrogen bonds are shown as orange dashed lines with lengths indicated in Å. (*c*) Hydrogen-bonding interactions in the 37–46 loop (60s loop) in DK-MTP-1P enolase. Bs-DK-MTP-1P and Gk-DK-MTP-1P enolases are shown in the same colours as in (*a*). The side chains of the residues involved in hydrogen bonds in the 60s loop of DK-MTP-1P enolase are represented as sticks. The colour coding is the same as in (*b*).

Table 3
Hydrogen bonds to residues in the 37–46 loop in DK-MTP-1P enolase.

Active state	Interacting atoms		Distance (Å)
E	Trp42 O	Ala44 N	3.1
		Leu45 N	3.4
ECM	Trp32 (42) O	Ala34 (44) N	3.1
		Leu35 (45) N	3.0
		Gln40 (50) $N^{\varepsilon 2}$	3.2
ECM-ligand	Trp32 (42) O	Ala34 (44) N	3.2
		Leu35 (45) N	3.1
		Gln40 (50) $N^{\varepsilon 2}$	3.2

On the other hand, the corresponding residue is substituted by Glu in Gk-DK-MTP-1P enolase and loop-6 of the E-PO_4^{3-} form of Gk-DK-MTP-1P enolase is in a disordered open conformation. These observations suggest that rigid constraints on the φ and ψ angles of Pro at position 338 may stabilize loop-6 in a closed conformation even if ligands are absent from the active site. In Bs-DK-MTP-1P enolase, the interactions between residues (Tyr306 and Arg313) on loop-6 and residues (Arg350 and Asp351) on a neighboring helix (α7) are found to stabilize the closed conformation of loop-6 (Fig. 5*b*); however, these residues are not conserved in the primary and tertiary structures of other RLPs. Therefore, Bs-DK-MTP-1P enolase may have a tendency to keep loop-6 in a closed conformation; this tendency is observed in several RLPs that feature a conserved Pro at position 338, but does not appear to be common to the other DK-MTP-1P enolases.

Unlike RuBisCO, the 37–46 loop, which is equivalent to the 60s loop (residues 61–70 in RuBisCO), is positioned about 15 Å away from the active site in the Bs-DK-MTP-1P and Gk-DK-MTP-1P enolases (Figs. 5*a* and 5*c*). This tendency can be seen in all available structures of RLPs. The primary structure of the 37–46 loop is less conserved within RLPs and the conformation of the 37–46 loop is mainly stabilized by main-chain hydrogen bonds (Fig. 5*c* and Table 3). Therefore, the unique conformation of the 37–46 loop in RLPs is not caused by RLP-specific amino-acid residues in the 37–46 loop. On the other hand, in RuBisCO the 60s loop is partially disordered in the E form and then becomes an ordered closed conformation in the ECM and ECM-ligand forms. The ordered conformation of the 60s loop is stabilized by an N-terminal extension (at positions 1–24 in Fig. 2) of RuBisCO, where seven amino-acid residues (Phe13, Lys14, Gly16, Val17, Lys18, Tyr20 and Tyr24) participate in a tight interaction with the 60s loop. Meanwhile, DK-MTP-1P enolases lack the corresponding N-terminal domain (Figs. 2, 3*b* and 3*d*). Although it cannot be ruled out that the functional residues (*e.g.* Glu60 and Thr65) in RuBisCOs may influence the conformation of the 60s loop, the lack of the N-terminal domain may be one reason for the unique structure of the 37–46 loop in DK-MTP-1P enolase.

This work was partly supported by the Research Fellowships of the Japan Society for the Promotion of Science for Young Scientists, the Science and Technology Incubation Program and the Global COE program from the Japanese Ministry of Education, Culture, Sports, Science and Technology to HT. This research was supported in part by a Core Research for Evolution Science and Technology (CREST) grant and the Science and Technology Incubation Program from the Japan Science and Technology Agency to TI and HM. The synchrotron-radiation experiments were performed at SPring-8 with the Institute for Protein Research, Osaka University (2006B6806). We are grateful to Professor A. Nakagawa, Dr E. Yamashita and Dr M. Yoshimura, Institute for Protein Research, Osaka University, at BL44XU (SPring-8) for their kind help in the data collection.

References

Andersson, I. (1996). *J. Mol. Biol.* **259**, 160–174.
Andrews, T. J. & Lorimer, G. H. (1987). *The Biochemistry of Plants*, edited by M. D. Hatch & N. K. Boardman, pp. 131–218. New York: Academic Press.
Ashida, H., Danchin, A. & Yokota, A. (2005). *Res. Microbiol.* **156**, 611–618.
Ashida, H., Saito, Y., Kojima, C., Kobayashi, K., Ogasawara, N. & Yokota, A. (2003). *Science*, **302**, 286–290.
Ashida, H., Saito, Y., Nakano, T., Tandeau de Marsac, N., Sekowska, A., Danchin, A. & Yokota, A. (2008). *J. Exp. Bot.* **59**, 1543–1554.
Badger, M. R. & Bek, E. J. (2008). *J. Exp. Bot.* **59**, 1525–1541.
Brünger, A. T., Adams, P. D., Clore, G. M., DeLano, W. L., Gros, P., Grosse-Kunstleve, R. W., Jiang, J.-S., Kuszewski, J., Nilges, M., Pannu, N. S., Read, R. J., Rice, L. M., Simonson, T. & Warren, G. L. (1998). *Acta Cryst.* D**54**, 905–921.
Carre-Mlouka, A., Mejean, A., Quillardet, P., Ashida, H., Saito, Y., Yokota, A., Callebaut, I., Sekowska, A., Dittmann, E., Bouchier, C. & de Marsac, N. T. (2006). *J. Biol. Chem.* **281**, 24462–24471.
Cleland, W. W., Andrews, T. J., Gutteridge, S., Hartman, F. C. & Lorimer, G. H. (1998). *Chem. Rev.* **98**, 549–562.
Collaborative Computational Project, Number 4 (1994). *Acta Cryst.* D**50**, 760–763.
Curmi, P. M., Cascio, D., Sweet, R. M., Eisenberg, D. & Schreuder, H. (1992). *J. Biol. Chem.* **267**, 16980–16989.
Duff, A. P., Andrews, T. J. & Curmi, P. M. (2000). *J. Mol. Biol.* **298**, 903–916.
Emsley, P. & Cowtan, K. (2004). *Acta Cryst.* D**60**, 2126–2132.
Hansen, S., Vollan, V. B., Hough, E. & Andersen, K. (1999). *J. Mol. Biol.* **288**, 609–621.
Hanson, T. E. & Tabita, F. R. (2001). *Proc. Natl Acad. Sci. USA*, **98**, 4397–4402.
Hartman, F. C. & Harpel, M. R. (1994). *Annu. Rev. Biochem.* **63**, 197–234.
Imker, H. J., Fedorov, A. A., Fedorov, E. V., Almo, S. C. & Gerlt, J. A. (2007). *Biochemistry*, **46**, 4077–4089.
Imker, H. J., Singh, J., Warlick, B. P., Tabita, F. R. & Gerlt, J. A. (2008). *Biochemistry*, **47**, 11171–11173.
Jones, T. A., Zou, J.-Y., Cowan, S. W. & Kjeldgaard, M. (1991). *Acta Cryst.* A**47**, 110–119.
Kraulis, P. J. (1991). *J. Appl. Cryst.* **24**, 946–950.
Kunst, F. *et al.* (1997). *Nature (London)*, **390**, 249–256.
Laskowski, R. A., MacArthur, M. W., Moss, D. S. & Thornton, J. M. (1993). *J. Appl. Cryst.* **26**, 283–291.
Leslie, A. G. W. (2006). *Acta Cryst.* D**62**, 48–57.
Li, H., Sawaya, M. R., Tabita, F. R. & Eisenberg, D. (2005). *Structure*, **13**, 779–789.
Lorimer, G. H. (1981*a*). *Annu. Rev. Plant Biol.* **32**, 349–383.
Lorimer, G. H. (1981*b*). *Biochemistry*, **20**, 1236–1240.
Lorimer, G. H., Chen, Y. R. & Hartman, F. C. (1993). *Biochemistry*, **32**, 9018–9024.
Lorimer, G. H. & Miziorko, H. M. (1980). *Biochemistry*, **19**, 5321–5328.

Lundqvist, T. & Schneider, G. (1991*a*). *J. Biol. Chem.* **266**, 12604–12611.
Lundqvist, T. & Schneider, G. (1991*b*). *Biochemistry*, **30**, 904–908.
Merritt, E. A. & Murphy, M. E. P. (1994). *Acta Cryst.* D**50**, 869–873.
Miziorko, H. M. & Sealy, R. C. (1980). *Biochemistry*, **19**, 1167–1171.
Mizohata, E., Matsumura, H., Okano, Y., Kumei, M., Takuma, H., Onodera, J., Kato, K., Shibata, N., Inoue, T., Yokota, A. & Kai, Y. (2002). *J. Mol. Biol.* **316**, 679–691.
Newman, J. & Gutteridge, S. (1993). *J. Biol. Chem.* **268**, 25876–25886.
Newman, J. & Gutteridge, S. (1994). *Structure*, **2**, 495–502.
Okano, Y., Mizohata, E., Xie, Y., Matsumura, H., Sugawara, H., Inoue, T., Yokota, A. & Kai, Y. (2002). *FEBS Lett.* **527**, 33–36.
Pierce, J. & Reddy, G. S. (1986). *Arch. Biochem. Biophys.* **245**, 483–493.
Saunders, N. F. (2003). *Genome Res.* **13**, 1580–1588.
Schneider, G., Lindqvist, Y. & Brändén, C. I. (1992). *Annu. Rev. Biophys. Biomol. Struct.* **21**, 119–143.
Schneider, G., Lindqvist, Y. & Lundqvist, T. (1990). *J. Mol. Biol.* **211**, 989–1008.
Schreuder, H. A., Knight, S., Curmi, P. M., Andersson, I., Cascio, D., Brändén, C. I. & Eisenberg, D. (1993). *Proc. Natl Acad. Sci. USA*, **90**, 9968–9972.
Shibata, N., Inoue, T., Fukuhara, K., Nagara, Y., Kitagawa, R., Harada, S., Kasai, N., Uemura, K., Kato, K., Yokota, A. & Kai, Y. (1996). *J. Biol. Chem.* **271**, 26449–26452.
Sugawara, H., Yamamoto, H., Shibata, N., Inoue, T., Okada, S., Miyake, C., Yokota, A. & Kai, Y. (1999). *J. Biol. Chem.* **274**, 15655–15661.
Suh, S. W., Cascio, D., Chapman, M. S. & Eisenberg, D. (1987). *J. Mol. Biol.* **197**, 363–365.
Tabita, F. R., Hanson, T. E., Li, H., Satagopan, S., Singh, J. & Chan, S. (2007). *Microbiol. Mol. Biol. Rev.* **71**, 576–599.
Tabita, F. R., Satagopan, S., Hanson, T. E., Kreel, N. E. & Scott, S. S. (2008). *J. Exp. Bot.* **59**, 1515–1524.
Tamura, H., Ashida, H., Koga, S., Saito, Y., Yadani, T., Kai, Y., Inoue, T., Yokota, A. & Matsumura, H. (2009). *Acta Cryst.* F**65**, 147–150.
Taylor, T. C. & Andersson, I. (1997*a*). *J. Mol. Biol.* **265**, 432–444.
Taylor, T. C. & Andersson, I. (1997*b*). *Biochemistry*, **36**, 4041–4046.
Taylor, T. C., Backlund, A., Bjorhall, K., Spreitzer, R. J. & Andersson, I. (2001). *J. Biol. Chem.* **276**, 48159–48164.
Taylor, T. C., Fothergill, M. D. & Andersson, I. (1996). *J. Biol. Chem.* **271**, 32894–32899.
Vagin, A. & Teplyakov, A. (1997). *J. Appl. Cryst.* **30**, 1022–1025.
Winans, S. C. & Bassler, B. L. (2002). *J. Bacteriol.* **184**, 873–883.
Zhang, K. Y., Cascio, D. & Eisenberg, D. (1994). *Protein Sci.* **3**, 64–69.